Available online at www.sciencedirect.com

ScienceDirect

Procedia Engineering 90 (2014) 327 – 332

Procedia Engineering

www.elsevier.com/locate/procedia

10th International Conference on Mechanical Engineering, ICME 2013

Effects of low Reynolds number on decay exponent in grid turbulence

Md Kamruzzaman*, L.Djenidi, R.A. Antonia

** Department of Mechanical Engineering, The University of Newcastle-2308, Australia*

Abstract

This present work is to investigate on the decay exponent (n) of decay power law ($q'^2 \sim (t-t_o)^n$, q'^2 is the total turbulent kinetic energy, t is the decay time, t_0 is the virtual origin) at low Reynolds numbers based on Taylor microscale $R_\lambda (\equiv u'\lambda/\nu) \le 64$. Hot wire measurements are carried out in a grid turbulence subjected to a 1.36:1 contraction. The grid consists in large square holes (mesh size 43.75 mm and solidity 43%); small square holes (mesh size 14.15mm and solidity 43%) and woven mesh grid (mesh size 5mm and solidity 36%). The decay exponent (n) is determined using three different methods: (i) decay of q'^2, (ii) transport equation for ε, the mean dissipation of the turbulent kinetic energy and (iii) λ method (Taylor microscale $\lambda \equiv \sqrt{5\langle q'^2 \rangle / \langle \varepsilon_d \rangle}$, angular bracket denotes the ensemble). Preliminary results indicate that the magnitude n increases while $R_\lambda (\equiv u'\lambda/\nu)$ decreases, in accordance with the turbulence theory.

Keywords: Initial conditions; turbulent kinetic energy (q'^2); mean dissipation energy rate (ε); Taylor microscale (λ); Taylor microscale Reynolds number (R_λ); and decay exponent (n).

Selection and peer-review under responsibility of the Department of Mechanical Engineering, Bangladesh University of Engineering and Technology (BUET)

Nomenclature

q'^2	Turbulent kinetic energy
n	Decay exponent
R_λ	Reynolds number based on Taylor microscale
t_o	Virtual origin
Greek symbols	
ε	Mean dissipation energy rate

* Corresponding author. Tel. +61-0435141454
E-mail address : MD Kamruzzaman@uon.edu.au

Selection and peer-review under responsibility of the Department of Mechanical Engineering, Bangladesh University of Engineering and Technology (BUET)
doi:10.1016/j.proeng.2014.11.857

λ	Taylor microscale
ν	Kinematic viscosity

1. Introduction

Grid turbulence is of great importance because it represents a close approximation to homogeneous isotropic turbulence. Such type of turbulence flow decays because there is no mean shear and no production of turbulent kinetic energy. It is produced by placing a grid (for example, perforated plate as in this study) of identical mesh in a uniform flow. Its study is of considerable interest since the work of Taylor (1935b), due to its simplicity and as a support in understanding the fundamental properties of turbulent flows. Similarity analysis and universal behavior of turbulence are studied by [1] and [2]. The decay of the turbulent kinetic energy (hereafter, TKE) q'^2 (a prime denotes the root-mean-square value), follows a power law $q'^2 \sim t^n$, where $n < 0$, the actual value of n at R_λ below 10 has yet to be determined. [3] indicates $n = -2.5$ and [4] predicts $n = -1.5$ at the low Reynolds number for the final period of decay. [5] mentioned that n may not be universal at the finite Reynolds. [6, 7, 8] have found that $1.16 \le n \le 1.37$. [9] and [10] collected a large number of velocity data points over a large wide downstream range to determine n more accurately. It was found that n depend on the initial conditions (i.e. grid geometry and Reynolds number) [9]. [11] used the contraction behind the grid to reduce the intensity of vortex shedding and anisotropy of the flow as well as these is effect on the decay exponent. Velocity fluctuation near the grid where the flow is inhomogeneous and anisotropic and the decay power law is inapplicable [12].

The purpose of the present study is to investigate the decay exponent at low Reynolds numbers in grid turbulence with focus at very low value of R_λ.

2 Experimental apparatus

Figure 1 shows the two different perforated grids. The first (Lsq43) is a grid of large square perforated with mesh size 43.75mm and second (Ssq43) is a small square perforated grid with mesh size 14.15mm. The solidity of first two turbulence generating grid is $\sigma = 43\%$. Mesh ratio of Lsq43 to Ssq43 is 3:1 approximately. The third grid is the woven mesh grid (WMG 36) and its solidity $\sigma = 36\%$.

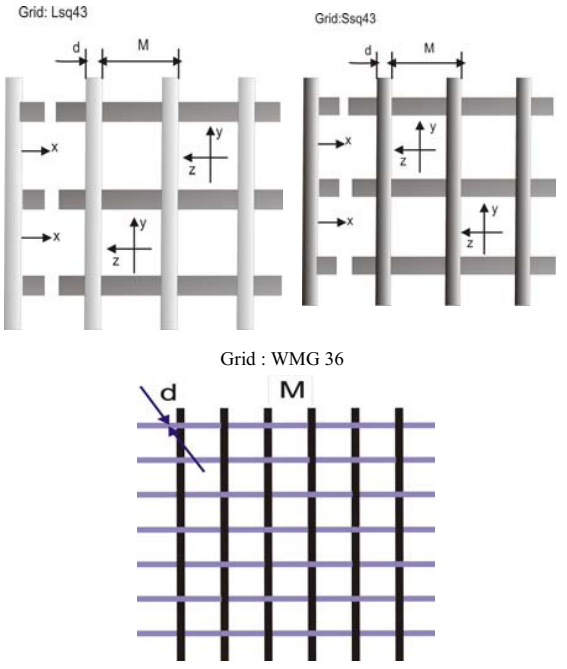

Fig. 1. The geometry of two different perforated grids and one woven mesh grid, mesh solidity is $\sigma = d/M(2 - d/M)$; x coordinates axis lies on the centreline of duct.

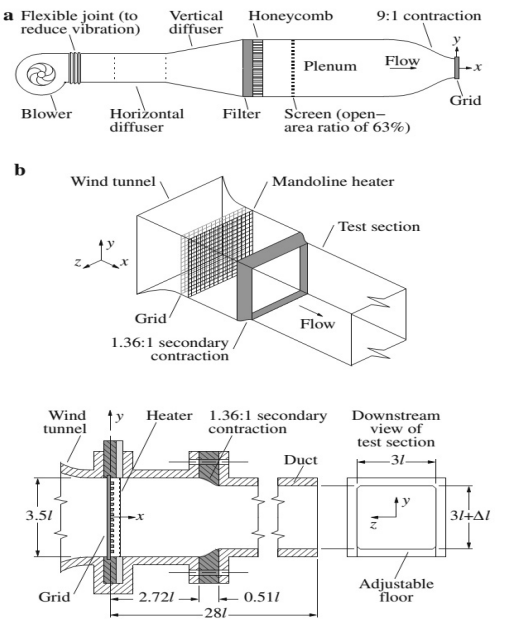

Fig. 2. a) The wind tunnel. b) The test section with the 1.36:1 secondary contraction downstream of the grid (scale: $l = 0.1m$).

Figure 2 shows a schematic diagram of the open circuit wind tunnel that [9] previously used. The air flow is driven by a centrifugal blower which is controlled by a variable-cycle (0-1,500 rpm) power supply. To minimize vibration, the blower is supported by dampers and is connected to the tunnel by a flexible joint. At the inlet to the platinum, an air filter (594 mm × 594 mm × 96 mm long) captures particles from the flow and a honeycomb ($l/d \approx 4.3$) removes residual swirl. A wire screen (with an open area ratio of 63%) and a smooth 9:1 primary contraction in the plenum improve the uniformity of the flow. For the arrangement of the secondary (1.36:1) contraction shown in Fig. 2, the inlet plane of the contraction is at x/M=6.2 and 19.2 in case of two different grids downstream of the grid. The velocity along the working section i.e. duct is not constant and the time t required for turbulence to be convected from the grid at say's=0 to a downstream position's=x' (e.g. [9], [11], [12) is given by

$$t = \int_0^x \frac{ds}{\langle U(s) \rangle} \quad (1)$$

where the mean velocity <U(x)> is approximated by the centreline velocity $U_{cl}(x)$ of the wind tunnel flow in the absence of the grid. The angular brackets denote the mean value. From Fig. 3, the centreline velocity is measured by using a Pitot-satic tube and a 100-pa micro-manometer.

For this study, the grid-mesh Reynolds number is investigated at two different speeds at 4.6m/s and 6.4m/s. The mesh size of two grids are different, so that $R_M = MU_o/\nu =$ 1474, 4170, 5800, 12900 and 17950 respectively. The Taylor microscale Reynolds number, $R_\lambda = u'\lambda/\nu$ are in the range between 7 and 64.

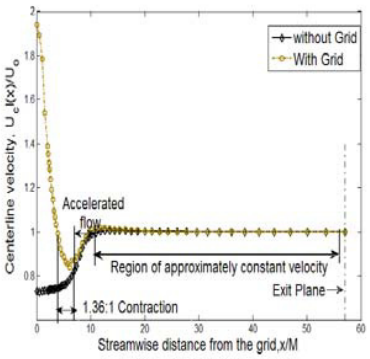

Fig. 3. Centreline distribution of wind tunnel Velocity.

3 Measurement technique

The velocity fluctuation (u) have measured simultaneously using a "hot-wire" probe. The hot wire (diameter $d \approx 2\mu m$; length $l = 200\,d$) is etched from a coil of Wollaston (Platinum). The hot wire measurements are carried out in two different wire configuration (single and cross hot wire) and hot wire operated with an ambient constant temperature anemometer (hereafter, CTA) with an over-heat ratio of 1.5. The output signal from CTA circuits passed from the gain units, offset and low pass filtered at a cut –off frequency f_c close to the Kolmogorov frequency f_k ($\equiv U_o/2\pi\eta, \eta = \nu^{3/4}\langle\varepsilon\rangle^{-1/4}$ is the Kolmogorov length scale). Sampling frequency is at least twice or greater than two times of cut-off frequency, [13] (see, Nyquist frequency theory). The hot-wire signals were digitized into a personal computer with a ±10 V and 16 bit analogue-digital converter.

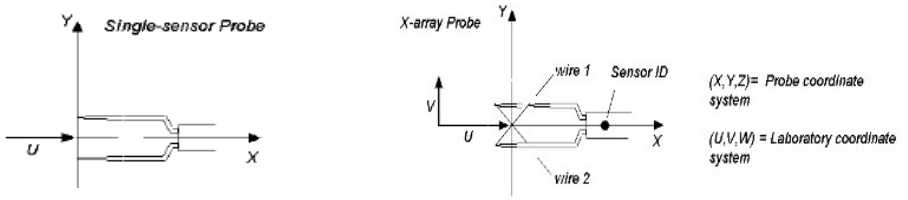

Fig. 4. Geometric configuration of hot wire probes (a) Single probe and (b) Cross probe.

4 Methods of decay power law in grid turbulence

In freely decaying turbulent flow and the decay of TKE follows a power law:

$$q'^2 \propto (t - t_o)^n \quad (2)$$

where, t_o is the virtual origin if decaying in time. When TKE decay through the space and (2) can be written as

$$q'^2 \propto (x-x_o)^n \text{, where, } x_o \text{ is the virtual origin if decaying in space} \quad (3)$$

However, The velocity is not constant in working section of the wind tunnel because of secondary contraction in this present study (see Figure 3) and the time is to be convected from the grid to the downstream location x, thus the more appropriate definition of TKE power law is given by [9,11, 12] . In grid turbulence one can be write the decay power law

$$q'^2 = A\left(\frac{tU_o}{M}-\frac{t_oU_o}{M}\right)^n \quad (4)$$

where, the Taylor hypotheses (i.e. $x = U_o t$) is used. Grid turbulence with contraction has been studied recently by [9] and established that the turbulence flow is nearly isotropic .The turbulent kinetic energy q'^2 and root-mean square of velocity fluctuation u'^2 exhibits a power-law decay rate, where their decay rates are about the same. The relation (4) can be used to determine the mean turbulent kinetic energy dissipation $\langle \varepsilon_d \rangle$ is a quantity which can be expressed in-terms of TKE budget and it is notoriously difficult to measure. The prefix'd' refers the decay of energy.

$$\langle \varepsilon_d \rangle = -\frac{U_o}{2}\frac{d\langle q'^2\rangle}{dx} = -\frac{U_o}{2}\left(1+\frac{2}{r_{uw}}\right)\frac{du'^2}{dx} \quad (5)$$

Here, r_{uw} is the ratio of u'^2/w'^2, where w' is the lateral fluctuation of the turbulence flow. The general definition of the Taylor microscale λ and Taylor microscale Reynolds number R_λ, which avoid the uncertainty that are arises from the directional dependence of $\langle (\partial u/\partial x)^2 \rangle$ and $\langle u^2 \rangle$ are used in this present study.

$$\lambda^2 = 5\nu\frac{\langle q'^2\rangle}{\langle \varepsilon_d \rangle} \text{ and } R_\lambda = \frac{\langle q'^2\rangle^{1/2}\lambda}{3^{1/2}\nu} \quad (6)$$

Using (4), then (5) and (6) can be rearranged to give

$$\langle \varepsilon_d \rangle = -\frac{UAn}{2M}\left(\frac{tU_o}{M}-\frac{t_oU_o}{M}\right)^{n-1} \quad \text{and} \quad \lambda^2 = -\frac{10M\nu}{Un}\left(\frac{tU_o}{M}-\frac{t_oU_o}{M}\right) \quad (7)$$

In the present study, n is obtained independently from (4) and (7) by measuring q', ε_d and λ

5 Results and discussion

The analysis begins by selecting virtual origin. The virtual origin was estimated using a trial and error method adopted by [11]. Different choices of t_o were applied and the ratios of $\lambda^2/U_o(t-t_o)$ are plotted in Fig. 5 and best straight lines indicate the virtual origin for different choices of $U_o t_o / M$. The determination technique of the virtual origin for all three different grids has been shown in Fig. 5. (a-e).

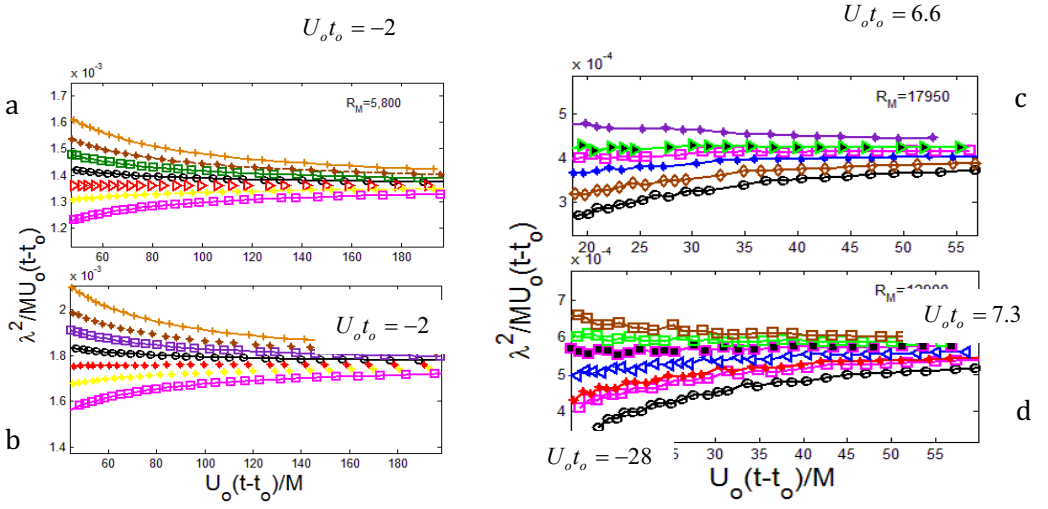

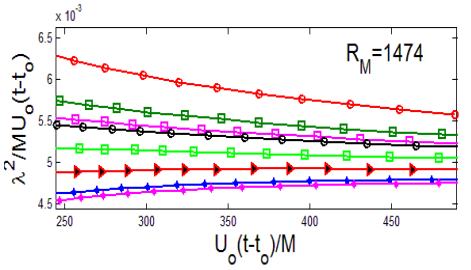

Fig. 5. Ratio of λ^2 with $U_o(t-t_o)/M$ for different choices of $U_o t_o / M$. (a, b) Small square Grid ; (c,d) Large square grid; (e) Woven mesh grid .

Figure 6 (a), shows q'^2 and $\langle \varepsilon_d \rangle$ decays along to the downstream position with adjustment of the virtual origin for $R_M = 5800$ and 4170 respectively where the mesh size is 14.15 mm. It is clear that both q'^2 and $\langle \varepsilon \rangle$ follow a power law with $n_q = -1.36$ and -1.26, $n_\varepsilon = -2.36$ and -2.26 . The large square perforated grid gives the decay exponents rate $n_q = -1.15$ and -1.14 according to the relation (4) which is shown in Fig. 6 (b). Mean energy dissipation rate of large perforated grid also follows the relation (7) and provides decay exponents rate $n_\varepsilon = -2.15$ and -2.14 . Measurements have been carried out with a large square grid at different Reynolds number based on mesh size ($M = 43.75\ mm$) 12900 and 17950 respectively. The Women mesh grid also provides the $n_q = -1.50$ and $n_\varepsilon = -2.50$ where, $R_M = 1474$.

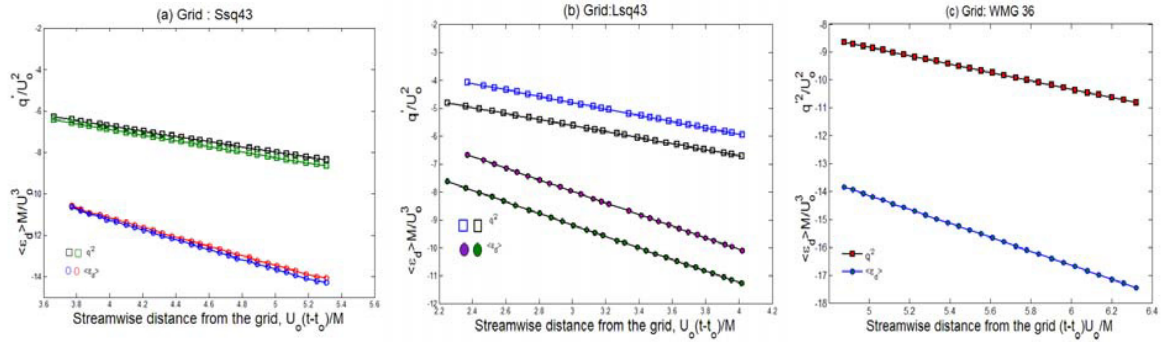

Fig. 6. The power law of turbulent kinetic energy, q'^2 and its mean dissipation rate, $\langle \varepsilon_d \rangle$, downstream of each grid with adjustment for optimum virtual origin $U_o t_o / M$ (a) Small square perforated grid ;(b) Large square perforated grid; (c) Woven mesh grid (WMG).

The decay rates of Taylor microscale n_λ is consistent with the decay rates of turbulent kinetic energy n_q which are given in Table 1. It is very clear that from the Table 1 that the decay exponent (n) is a function of R_M . It is also consider that the magnitude of n increases as R_λ decreases.

Table 1. Decay exponents of Lsq43, Ssq43 and WMG 36. The "Taylor microscale" method is used to determine the optimum virtual origin ($U_o t_o / M$).

Grids	Initial Condition	U_o	$U_o t_o / M$	$-n_q$	$-n_\varepsilon$	$-n_\lambda$	R_λ	R_M
Lsq43	1.36:1	6.4 m/s	6.6	1.14	2.14	1.14	65-58	17900
	Contraction	4.6 m/s	7.3	1.15	2.15	1.15	50-45	12950
Ssq43	1.36:1	6.4 m/s	-2.0	1.26	2.26	1.16	30-23	5800
	Contraction	4.6 m/s	-2.0	1.36	2.36	1.36	23-17	4170
WMG36	1.36:1	4.6 m/s	-28.0	1.50	2.50	1.50	10-7	1474
	Contraction							

Figure 7 shows the variation of n with R_λ . Decay exponent $(n) \approx 1.14$ for relatively high R_λ also obtained by [9]. R_λ decreases there is a clear increase in the magnitude of n_q , thus the trend is consistent with the theory of turbulence, which predicts that $|n|$ reaches a maximum when $R_\lambda \to 0$. For example, a value of decay exponent rate $n = -2.5$ is predicted according to Batchelor in the decay of final period [14]. According to Saffman decay-like, a value of $n = -1.5$ is expected (e.g. [4]). At this stage it is not clear, which limit of decay exponent (n) is correct, as some data are required to a lower R_λ . Decay exponent $(n_q) = -1.5$ has obtained in the present investigation at low $R_\lambda \approx 7$, which is consistent with Saffman decay exponent.

6 Conclusion

The present study describes the effect of low Reynolds number R_λ on the decay exponent rates in grid turbulence. Experiments with two different turbulence generating grids show that the velocity fluctuations follow power law decay and decay exponent rate (n) depends on the grid geometry. It has found that n are in the range -1.50 to -1.14 , but n increases as R_λ decreases for example $n \approx -1$ when $R_\lambda \to \infty$. Experiment will be carried on towards to the small $R_\lambda \to 0$ as a future work in a final period of decay region in grid turbulence.

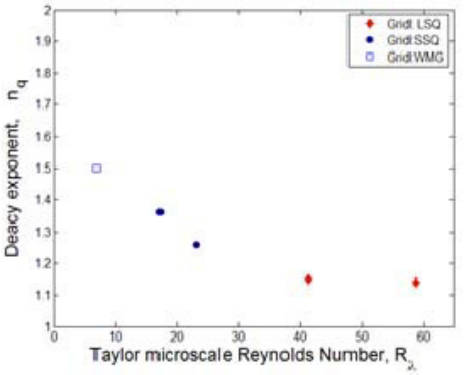

Fig. 7. Decay exponent (n) decreasing function of Taylor micro-scale Reynolds numbers R_λ .

References

[1] Kármán, T., Howarth, L., 1938. On the statistical theory of isotropic turbulence, Proc. R. Soc. Lond Ser A Math Phys Sci 164(917), 192-215.
[2] Dryden, H.L., 1943. A review of the statistical theory of turbulence, Quart. Appl. Math. 1, 7-42.
[3] Batchelor, G.K., 1953. The theory of homogeneous turbulence, Cambridge University Press, Cambridge.
[4] Saffman, P.G., 1967. The large scale structure of homogeneous turbulence, Journal of Fluid Mechanics 27(3), 581-593.
[5] George, W.K., 1992b. The decay of homogeneous isotropic turbulence, Physics of Fluids 4(7), 1492-1509.
[6] Corrsin, S., 1963. Turbulence: experimental methods. In Handbuch der Physik (ed. S.Flügge and C.A. Truesdell) pp. 524-589, Springer.
[7] Comte-Bellot, G., Corrsin, S., 1971. Simple Eulerian time correlation of full-and narrow –band velocity signals in grid generated, ‘ isotropic’ turbulence. Journal of Fluid Mechanics, 25, 657-682.
[8] Uberoi, M.S., Wallis, S., 1967. Effect of grid geometry on the turbulence decay, Physics of Fluids10, 1216-1224.
[9] Lavoie, P., 2006. Effects of initial conditions in decaying grid turbulence. Ph.D. Thesis, University of Newcsatle, Newcastle, Australia.
[10] Krogstad, P.Å., Davidson, P.A., 2010. Is grid turbulence Saffman turbulence?, Journal of Fluid Mechanics 624, 373-394.
[11] Comte-Belloot, G., Corrsin, S., 1966. The use of a contraction to improve the isotropy of grid generated turbulence, Journal of Fluid Mechanics 25, 657-682.
[12] Mohamed, M.S., LaRue, J., 1990. The decay power law in grid generated turbulence, Journal of Fluid Mechanics, 219, 195-214.
[13] Stanley, W.D., 1975. Digital signal processing, Reston publishing company, inc., Reston, Virginia.
[14] Batchelor, G.K., Townsend, A.A., 1948b. Decay of turbulence in the final period, Proc. R. Soc. London,Ser. A 194, 527-543.